Table 1 | Relationship between overproduction hyperuricemia and ABCG2 dysfunction.

Estimated transport activity	Genotype		N		Frequency of OP hyper-uricemia	RR	95% CI	P	Adjusted RR†	Adjusted 95% CI†	Adjusted P†
	Q126X (rs72552713)	Q141K (rs2231142)	OP hyper-uricemia*	Non-OP hyper-uricemia*							
≤1/4 Function	X/X Q/X	Q/Q Q/K	26	3	0.897	2.35	1.86–2.97	3.32×10^{-7}	2.30	1.31–3.90	2.65×10^{-3}
1/2 Function	Q/X Q/Q	Q/Q K/K	96	55	0.636	1.66	1.32–2.10	8.58×10^{-6}	1.79	1.25–2.59	1.55×10^{-3}
3/4 Function	Q/Q	Q/K	160	147	0.521	1.36	1.09–1.71	4.55×10^{-3}	1.42	1.03–2.00	0.035
Full function	Q/Q	Q/Q	60	97	0.382	1.00					

Abbreviations: CI, confidence interval; OP, overproduction; RR, risk ratio.
*Patients were classified as OP hyperuricemia (OP type and combined type) when their UUE was over 25.0 mg h^{-1}/1.73 m^2 (600 mg per day/1.73 m^2). UUE was normalized for a body surface area of 1.73 m^2. Other patients were classified as non-OP hyperuricemia.
†Using Poisson regression analysis, RR, 95% CI, and *P* value are adjusted with covariates of body mass index, alcohol intake, and single nucleotide polymorphisms of urate-related genes (rs506338 in *URAT1*, rs11722228 in *GLUT9* and rs12129861 in *PDZK1*).

the risk of 'overproduction' hyperuricemia, conferring a risk ratio (RR) of 2.35 (95% CI 1.86–2.97; $P=3.32\times10^{-7}$) (Table 1). In addition, moderate and mild dysfunction also significantly increased the risk of 'overproduction' hyperuricemia, conferring an RR of 1.66 (95% CI 1.32–2.10; $P=8.58\times10^{-6}$) and 1.36 (95% CI 1.09–1.71; $P=4.55\times10^{-3}$), respectively. Risk of overproduction hyperuricemia was still significant after adjustment (Table 1). These results clearly demonstrate that ABCG2 dysfunction increases UUE, thereby leading to increased frequency of 'overproduction' hyperuricemia. This seems paradoxical in light of the current concept of hyperuricemia, but it would be understandable if extra-renal excretion via ABCG2 has a physiologically significant role in urate regulation.

Abcg2 dysfunction and urate excretion in mice. Next, we investigated how ABCG2 dysfunction affected the urate excretion pathways and re-evaluated the current concept of hyperuricemia based on ABCG2 dysfunction. The evaluation of gut urate excretion in humans is intrinsically difficult because urate excreted into the intestinal lumen is rapidly metabolized by bacterial flora. To solve this problem, we introduced an animal model in which urate excretion through the gut is easily achievable by invasive sampling. Also, *Abcg2*-knockout mice were treated with oxonate, a uricase inhibitor, so that the urate metabolism of this model mimicked that of humans that lacks the urate degrading enzyme, uricase[22]. First, mouse Abcg2 is revealed to mediate urate transport (Fig. 3a) using the membrane vesicle system prepared from HEK293 cells that express mouse Abcg2. The export process by mouse Abcg2 was ATP-dependent and not saturable under the physiological concentration of urate (Fig. 3a), indicating high-capacity urate transport activity by Abcg2. Another functional analysis demonstrated that oxonate has no hazardous effect on the Abcg2-mediated urate transport (Fig. 3b). We then tried to characterize the excretion of urate into urine, bile and intestinal lumen using the *in vivo* mouse model. As shown in Fig. 3c, SUA of *Abcg2*-knockout mice was significantly higher than that of control mice ($P=8.8\times10^{-6}$), which is consistent with the increase of SUA in humans with ABCG2 dysfunction[21]. Under this condition, the urinary urate/creatinine ratio was significantly increased in *Abcg2*-knockout mice ($P=4.1\times10^{-4}$) (Fig. 3d), which also corroborates the observation in humans (Fig. 2a). On the other hand, the urate excretion from the intestine was significantly lower in *Abcg2*-knockout mice (Fig. 3e), which is supported by the similar results of the transintestinal urate transport experiment (Fig. 3f; Supplementary Fig. S2). Calculated velocity of the intestinal urate excretion in *Abcg2*-knockout mice was less than a half of that in control mice ($P=3.6\times10^{-4}$) (Fig. 3g), whereas biliary urate excretion showed no significant difference regardless of *Abcg2* genotype (Fig. 3g). From these results, we estimated the relative contribution of each pathway to the total urate excretion; in wild-type mice, the UUE pathway contributes approximately two-thirds, and the intestinal excretion pathway contributes one-third of the total urate excretion, whereas the urate excretion into bile is 2.2% of the total urate excretion (Fig. 3h). The ratio of each urate excretion pathway is consistent with the previous literature about the estimation of urate excretion pathways in humans[4,5]. As a result of decreased intestinal excretion, the urate excretion in *Abcg2*-knockout mice was much more dependent on the urinary excretion pathway (Fig. 3h). Furthermore, the small contribution of biliary urate excretion in mice (Fig. 3h) is also consistent with a report of human urate excretion, which shows that biliary urate excretion consists of less than 5 percent of the total urate excretion[23]. Taken together, ABCG2 is suggested to have an important role in extra-renal urate excretion, especially in intestinal urate excretion. Accordingly, increased SUA in patients with ABCG2 dysfunction can be explained by the decreased excretion of urate from the intestine.

Discussion

We found that the decrease in urate exporter ABCG2 function in hyperuricemic patients is associated with the increase of UUE and frequency of overproduction hyperuricemia, which consists of the overproduction type and the combined type. Also, any ABCG2 dysfunction caused by common dysfunctional variants significantly raised the risk of overproduction hyperuricemia. *Abcg2*-knockout mice treated with oxonate showed increased renal urate excretion as well as SUA and decreased intestinal urate excretion, compared with those of wild-type mice. These findings indicate that the decrease in extra-renal urate excretion via dysfunctional ABCG2 is a common mechanism of hyperuricemia, which has been currently mistaken for urate 'overproduction' due to increased UUE.

Three main transporters have been confirmed to regulate SUA in humans; a secretion transporter ABCG2 and two urate reabsorption transporters, URAT1 (ref. 10) and GLUT9 (refs 14,15). In addition, urate transporters including ABCG2 and URAT1 are regulated

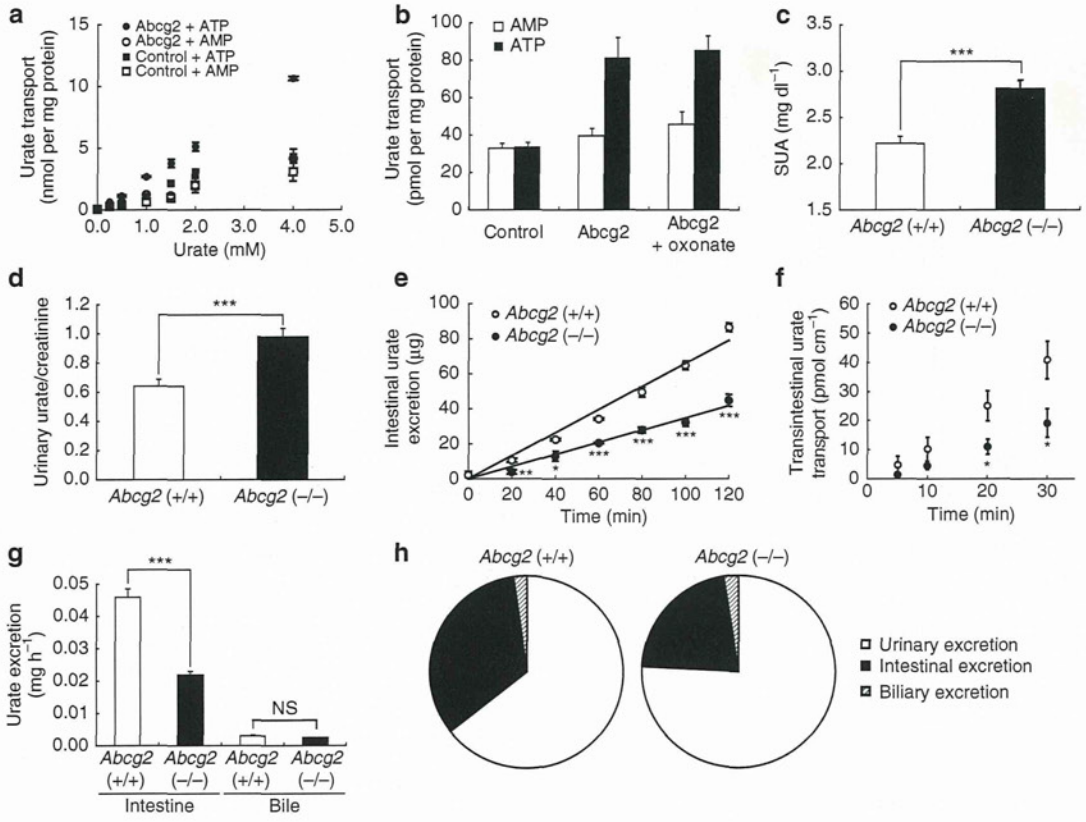

Figure 3 | Urate excretion via Abcg2 in a mouse model. (**a**) Concentration-dependent urate transport via Abcg2 ($n=3$). (**b**) Effect of oxonate on Abcg2-mediated urate transport ($n=3$). (**c**–**e**, **g**, **h**) *In vivo* study using *Abcg2*-knockout and wild-type mice. (**c**) Serum uric acid (SUA) levels ($n=19$–20). $^{***}P=8.8\times10^{-6}$. (**d**) Urinary excretion of urate ($n=10$–11). $^{***}P=4.1\times10^{-4}$ (**e**) Time course of intestinal urate excretion ($n=4$). $^{***}P<0.001$; $^{**}P=0.0066$; $^{*}P=0.021$. (**f**) Transintestinal urate transport ($n=3$–4). $^{*}P=0.037$ and 0.034 for 20 min and 30 min, respectively. (**g**) Urate excretion in intestine and bile ($n=3$–4). $^{***}P=3.6\times10^{-4}$. All bars show means±s.e.m. *P* values were obtained by Student's *t*-test. NS, not significant. (**h**) Relative contribution of urinary, intestinal and biliary urate excretion pathways.

by an adaptor protein, the PDZ domain containing-protein, PDZK1 (refs 24,25). Among these urate-related genes, dysfunctional variants of *ABCG2* are demonstrated as a major cause of gout and hyperuricemia[20,21]. ABCG2 is expressed on the apical membrane of several tissues including kidney[26], liver and intestine[27]. As ABCG2 is supposed to mediate renal urate excretion[20], the dysfunction of this molecule is expected to decrease UUE. The results in this study, however, show an opposite conclusion that the dysfunction of ABCG2 results in an increase of UUE. This contradiction can be explained by two facts: kidney is not the only organ in which ABCG2 is expressed[27,28], and one-third of urate excretion in humans depends on the extra-renal pathway such as gut excretion[4,5,8]. Also, together with little intestinal expression of URAT1 (ref. 10), our data from an animal model indicate that the decreased expression of Urat1 in the kidney could partially account for the increased urate in urine in *Abcg2*-knockout mice (Fig. 3d, Supplementary Fig. S3). Therefore, it is reasonable that common dysfunction of ABCG2 can cause a decrease of urate excretion via the extra-renal pathway rather than the renal pathway.

The current classification of hyperuricemia is based on the understanding of its mechanism by which hyperuricemia results from either overproduction of urate due to a metabolism disorder, underexcretion by abnormal renal urate transport activity, or the combination of the two. So far 'renal urate underexcretion' has been widely considered to be a main cause of hyperuricemia, and 'urate overproduction' is recognized as another common cause. A part of hyperuricemia is definitely attributable to lifestyle factors such as consumption of an excessive amount of alcohol as well as high-calorie diet intake. However, even taking such factors into account, most causes of 'overproduction' hyperuricemia still cannot be explained. Many attempts have been made to elucidate the pathogenesis of 'overproduction' hyperuricemia. Nevertheless, no study has succeeded in identifying the exact mechanism of urate overproduction except some urate metabolism disorders[29] including Lesch–Nyhan syndrome (hypoxanthine-guanine phosphoribosyl transferase deficiency), accelerated purine nucleotide degradation and accelerated ATP breakdown. Our findings indicate that a major cause of 'overproduction' hyperuricemia is not true overproduction of urate but rather 'extra-renal urate underexcretion' by common ABCG2 dysfunction. We also suggest that re-classification of hyperuricemia is necessary because 'overproduction' hyperuricemia in the current classification is only defined by the result of UUE value and does not represent a correct pathophysiological condition. Therefore, our data lend support to the idea that 'overproduction type' in the current classification of hyperuricemia should be renamed 'renal overload type,' which includes subtypes of 'extra-renal underexcretion' and genuine 'overproduction' (Fig. 4).

In this study, we suggest a common mechanism of hyperuricemia by decreased extra-renal excretion due to ABCG2 dysfunction. Therefore, ABCG2 could be a promising target for urate-lowering medications without adverse effects such as urolithiasis. Our findings and proposal would serve to correct the long-misunderstood

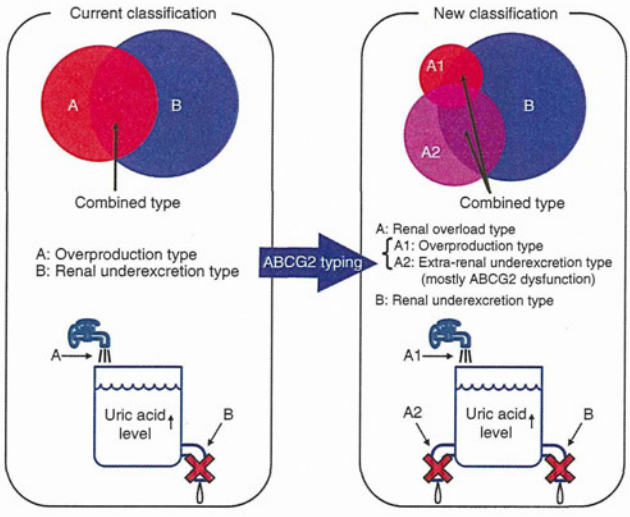

Figure 4 | Pathophysiological model and proposed new classification of hyperuricemia. Hyperuricemia is currently classified into urate 'overproduction type' (A), 'renal underexcretion type' (B), and combined type. Taking extra-renal urate excretion into account, we propose a testable model by which 'overproduction type' be renamed 'renal overload type' (A), consisting of two subtypes, genuine 'overproduction' (A1) and 'extra-renal underexcretion' (A2).

pathophysiology of hyperuricemia. This new concept will help pinpoint the causes of hyperuricemia more accurately and provide a more effective therapeutic strategy for hyperuricemia and gout, leading to a good model of personalized medicine for common diseases.

Methods

Study participants. This study was approved by the institutional ethical committees, and all procedures involved in this study were performed in accordance with the Declaration of Helsinki. Hyperuricemia patients were diagnosed when their SUAs were higher than 7.0 mg dl^{-1}, and gout cases were also clinically diagnosed as primary gout according to the criteria established by the American College of Rheumatology[30]. All hyperuricemic subjects and primary gouty patients were eligible, when written consent was obtained at the gout clinics of either Jikei University Hospital (Tokyo, Japan) or Midorigaoka Hospital (Osaka, Japan). The following patients were excluded; patients without information on clinical parameters shown in Supplementary Table S1, or those with inherited metabolism disorders including Lesch–Nyhan syndrome. Finally, 644 male outpatients, including 575 gout cases, were registered as valid participants.

Clinical parameters for urate handling. Clinical parameters including SUA, amount of UUE and fractional excretion of urate clearance (urate clearance/creatinine clearance ratio, FE_{UA}) were measured for each patient after diet education, concerning low-purine and calorie-controlled diet, as well as less fructose and alcohol intake[31,32]. Clinical parameters before taking medications for hyperuricemia were used in this study. Both UUE and FE_{UA} were calculated after a few-hour urine collection. UUE was normalized for a body surface area of 1.73 m^2. In this study, patients were classified as overproduction hyperuricemia when their UUE was over 25.0 mg h^{-1}/1.73 m^2 (600 mg day^{-1}/1.73 m^2)[7,8,33]. Those who had FE_{UA} under 5.5% were classified as underexcretion hyperuricemia[34] on the basis of the normal FE_{UA} range (5.5–11.1%)[35]. Combined type was classified when their UUE and FE_{UA} met the criteria of both overproduction and underexcretion hyperuricemia (Fig. 1). Patients who met the single criterion of overproduction hyperuricemia, excluding combined type, were defined as overproduction type.

Genetic analysis. Genomic DNA was extracted from whole peripheral blood cells[36]. Genotyping was performed by high-resolution melting analysis with a LightCycler 480 (Roche Diagnostics)[21], or by an allelic discrimination assay (Custom Taqman MGB, Applied Biosystems) with a 7700 detector (Applied Biosystems)[37]. To confirm their genotypes, more than 100 samples were subjected to direct sequencing with primers shown in Supplementary Table S5. DNA sequencing analysis was performed with a 3130×l Genetic Analyzer (Applied Biosystems)[21]. The export function of ABCG2 was then estimated from the combinations of *ABCG2* variants, rs72552713 (Q126X) and rs2231142 (Q141K), and divided into four functional groups[21]; that is, full function, 3/4 function (mild dysfunction), 1/2 function (moderate dysfunction) and ≤1/4 function (severe dysfunction).

Experimental assessment for urate excretion pathways. Mouse Abcg2 complementary DNA (GenBank accession number NM_011920) was inserted into the *Not* I site of pcDNA3.1(+) vector plasmid (Invitrogen), with a myc-tag sequence attached at the 5′-end. The wild-type human ABCG2 cDNA (GenBank accession number NM_004827) or mutated (Q126X and Q141K) ABCG2 cDNA was inserted into the *Nhe* I and *Apa* I sites of pcDNA3.1(+) vector plasmid, with a myc-tag sequence attached at the 5′-end[21]. To prepare membrane vesicles, HEK293 cells were transiently transfected with the expression vector for Abcg2/ABCG2 or empty vector (control) by FuGENE6 (Roche Diagnostics), according to the manufacturer's instructions. Forty-eight hours later, cells were collected and the membrane vesicles were isolated by a standard method with repeated centrifugation and homogenization[38]. After the expression of Abcg2 protein was confirmed by western blot analysis, the uptake studies of [^{14}C]urate (28 μM, American Radiolabeled Chemicals) were performed by a standard protocol for transport assays with membrane vesicles[39]. All other chemicals used in this study were commercially available and of reagent-grade.

Male *Abcg2*-knockout mice (FVB.129P2-Abcg2, Taconic) and control FVB mice of 27–33 g were fed 2.0% (w/w) potassium oxonate for more than 1 week, as reported earlier[40]. Concentrations of urate and creatinine in collected serum and urine samples were determined by QuantiChrom Uric Acid Assay Kit (Bioassay systems) and Creatinine Assay Kit (Cayman Chemical Company). To analyze the intestinal urate excretion, mice fasted-overnight were anaesthetized by intraperitoneal injection of urethane and cannulated with polyethylene tubing (Hibiki Size 8) (Kunii Co.) at the upper duodenum and the middle jejunum to make an intestinal loop at the upper half of the intestine. After the intestinal contents were removed by the slow infusion of saline and air, the efflux buffer (saline containing 0.3 mM potassium oxonate) was introduced into the intestinal loop, and both ends of the loop were closed with syringes. After the indicated periods, the efflux buffer in the loop was collected by syringes and urate concentrations were quantified. Intestinal urate excretion was calculated from the following equation:

$$\begin{aligned}[\text{Intestinal urate excretion}] = {} & [\text{Urate concentration in the intestinal loop}] \\ & \times [\text{Volume of efflux buffer in the intestinal loop}] \\ & \times [\text{Length of the whole small intestine}] \\ & / [\text{Length of the intestinal loop}]\end{aligned}$$

To investigate the biliary urate excretion, mice were anaesthetized by intraperitoneal injection of urethane, the cystic duct was ligated and a common bile duct fistula was created using a Teflon catheter (UT-03) (Unique Medical). Urate in the hepatic bile specimens collected for 3 h was examined. Relative contribution of urinary, intestinal and biliary excretion pathways was estimated by the comparison of the calculated velocity of each pathway, for which the amount of daily urine is assumed to be 2 millilitres. Protocols were performed according to accepted criteria for humane care of experimental animals and approved by the review board of our institution for animal studies.

Western blot analysis. For western blot analysis, 5 μg of membrane vesicles diluted with 2×SDS loading buffer was separated on a 10% SDS-polyacrylamide gel electrophoresis plate with a 3.75% stacking gel. Proteins were transferred electrophoretically onto an Immunobilon membrane (Millipore) using a blotter (Bio-Rad Laboratories) at 15 V for 1 h. The membrane was blocked with Tris-buffered saline containing 0.05% Tween 20 (TBS-T) and 3% bovine serum albumin (BSA) for 1 h at room temperature. After washing with TBS-T, the membrane was incubated for 1 h at room temperature in TBS-T containing 0.1% BSA and anti-ABCG2/BCRP antibody (BXP-53, Abcam) (1:500, 0.5 μg ml^{-1}) for the detection of ABCG2, or anti-Na^+/K^+-ATPase α antibody (Santa Cruz Biotechnology) (1:200, 1.0 μg ml^{-1}) as a loading control of membrane proteins. For detection, the membrane was allowed to bind to a horseradish peroxidase-labelled secondary antibody (GE Healthcare) diluted 5,000-fold in TBS-T containing 0.1% BSA for 1 h at room temperature. The enzyme activity was assessed using an ECL Prime Western Blotting Detection System (GE Healthcare) with a luminescent image analyzer (Bio-Rad).

Transintestinal urate transport experiment. To demonstrate the intestinal transport of urate, the upper third of mice intestine specimens was collected and enteral contents were carefully removed. Next, both ends of the specimens were connected with syringes and the luminal sides were filled with 5 ml of Ringer Buffer (93.4 mM NaCl, 6.2 mM KCl, 2.0 mM KH_2PO_4, 1.2 mM $MgSO_4$-$7H_2O$, 2.5 mM $CaCl_2$-$2H_2O$, pH 7.4, 37 °C). Then, the specimens were incubated with [^{14}C]urate (0.4 μM)-containing Ringer Buffer (pH 7.4, 37 °C), pre-bubbled with mixed gas (95% O_2 and 5% CO_2) for 30 min. After incubation with indicated periods, 200 μl of luminal buffer was sampled followed by the addition of the same aliquot of the buffer. Syringes

were slowly pumped every 2.5 min to thoroughly mix the luminal buffer (Supplementary Fig. S2).

Quantitative real-time PCR. To determine messenger RNA levels of genes involved in urate transport, mice kidney specimens were homogenized in RNA iso plus (Takara) and extracted RNA was reverse-transcribed with ReverTra Ace (Toyobo). Quantitative real-time PCR was performed using 2× SYBR GREEN (Stratagene) and Chromo4 (BIO-RAD) at 95 °C 10 min followed by 40 cycles at 95 °C for 15 s, 50 °C for 30 s, and 72 °C for 40 s. We used primers for *Abcg2* (sense and antisense primers were 5′-aagcatagggatggagctga-3′ and 5′-ctgtgcttgagtc caaacca-3′, respectively), *Urat1* (sense and antisense primers were 5′-atcatctccatgct gtgctg-3′ and 5′-aagtccacaatcccgatgag-3′, respectively), *Glut9* (sense and antisense primers were 5′-cggcctggctctcaaacttcgccg-3′ and 5′-ggcgaagacgaggaagcagt-3′, respectively), *Pdzk1* (sense and antisense primers were 5′-atataatgcctcagggcgtg-3′ and 5′-atggctggcgttctctacat-3′, respectively) and *β-actin* (sense and antisense primers were 5′-ccggaaggaaaactgacagc-3′ and 5′-gtggtggtgaagctgtagcc-3′, respectively).

Statistical analysis. Haplotype estimation was performed with the EM algorithm[41]. To investigate the association of ABCG2 functions and UUE, simple linear regression analysis was performed with UUE as a dependent variable and estimated function of ABCG2 as an independent variable. To evaluate the relationship between ABCG2 function and overproduction hyperuricemia, the risk ratio (RR) and its 95% CI were calculated by dividing the proportion of overproduction hyperuricemia in each function category by that in full function category. Poisson regression analysis was performed to obtain adjusted RR of ABCG2 dysfunction for overproduction hyperuricemia with possible confounding factors, such as body mass index, alcohol intake, single nucleotide polymorphisms of urate-related genes, rs11722228 (*GLUT9/SLC2A9*)[18], rs506338 (*URAT1/SLC22A12*)[18], and rs12129861(*PDZK1*)[17]. For all calculations in the statistical analysis, software R (version 2.8.1) (http://www.r-project.org/) and SPSS (version 16.0J for Windows) (SPSS) were used.

References

1. Feig, D. I., Kang, D. H. & Johnson, R. J. Uric acid and cardiovascular risk. *N. Engl. J. Med.* **359,** 1811–1821 (2008).
2. Edwards, N. L. The role of hyperuricemia in vascular disorders. *Curr. Opin. Rheumatol.* **21,** 132–137 (2009).
3. Yeldandi, A. V. *et al.* Human urate oxidase gene: cloning and partial sequence analysis reveal a stop codon within the fifth exon. *Biochem. Biophys. Res. Commun.* **171,** 641–646 (1990).
4. Sorensen, L. B. Role of the intestinal tract in the elimination of uric acid. *Arthritis Rheum.* **8,** 694–706 (1965).
5. Sica, D. A. & Schoolwerth, A. in *Brenner and Rector's The Kidney* (ed. B.M. Brenner) 645–649 (Saunders, 2004).
6. Boss, G. R. & Seegmiller, J. E. Hyperuricemia and gout. Classification, complications and management. *N. Engl. J. Med.* **300,** 1459–1468 (1979).
7. Becker, M. A. in *The Metabolic & Molecular Bases of Inherited Disease* (eds Charles R. Scriver, Barton Childs, Kenneth W. Kinzler, & Bert Vogelstein) 2513–2535 (McGraw-Hill, 2001).
8. Wortmann, R. L. in *Harrison's Principles of Internal Medicine* (eds Anthony S. Fauci *et al.*) 2444–2449 (McGraw-Hill, 2008).
9. Ichida, K., Hosoyamada, M., Hosoya, T. & Endou, H. in *Genetic Diseases of the Kidney* (ed. Richard P. Lifton) 653–662 (Academic Press, 2009).
10. Enomoto, A. *et al.* Molecular identification of a renal urate anion exchanger that regulates blood urate levels. *Nature* **417,** 447–452 (2002).
11. Li, S. *et al.* The GLUT9 gene is associated with serum uric acid levels in Sardinia and Chianti cohorts. *PLoS Genet.* **3,** e194 (2007).
12. Döring, A. *et al.* SLC2A9 influences uric acid concentrations with pronounced sex-specific effects. *Nat. Genet.* **40,** 430–436 (2008).
13. Vitart, V. *et al.* SLC2A9 is a newly identified urate transporter influencing serum urate concentration, urate excretion and gout. *Nat. Genet.* **40,** 437–442 (2008).
14. Anzai, N. *et al.* Plasma urate level is directly regulated by a voltage-driven urate efflux transporter URATv1 (SLC2A9) in humans. *J. Biol. Chem.* **283,** 26834–26838 (2008).
15. Matsuo, H. *et al.* Mutations in glucose transporter 9 gene SLC2A9 cause renal hypouricemia. *Am. J. Hum. Genet.* **83,** 744–751 (2008).
16. Dehghan, A. *et al.* Association of three genetic loci with uric acid concentration and risk of gout: a genome-wide association study. *Lancet* **372,** 1953–1961 (2008).
17. Kolz, M. *et al.* Meta-analysis of 28,141 individuals identifies common variants within five new loci that influence uric acid concentrations. *PLoS Genet.* **5,** e1000504 (2009).
18. Kamatani, Y. *et al.* Genome-wide association study of hematological and biochemical traits in a Japanese population. *Nat. Genet.* **42,** 210–215 (2010).
19. Cheng, L. S. *et al.* Genomewide scan for gout in Taiwanese aborigines reveals linkage to chromosome 4q25. *Am. J. Hum. Genet.* **75,** 498–503 (2004).
20. Woodward, O. M. *et al.* Identification of a urate transporter, ABCG2, with a common functional polymorphism causing gout. *Proc. Natl Acad. Sci. USA* **106,** 10338–10342 (2009).
21. Matsuo, H. *et al.* Common defects of ABCG2, a high-capacity urate exporter, cause gout: a function-based genetic analysis in a Japanese population. *Sci. Transl. Med.* **1,** 5ra11 (2009).
22. Fridovich, I. The competitive inhibition of uricase by oxonate and by related derivatives of s-triazines. *J. Biol. Chem.* **240,** 2491–2494 (1965).
23. Sorensen, L. B. & Levinson, D. J. Origin and extrarenal elimination of uric acid in man. *Nephron* **14,** 7–20 (1975).
24. Shimizu, T. *et al.* PDZK1 regulates breast cancer resistance protein in small intestine. *Drug Metab. Dispos.* **39,** 2148–2154 (2011).
25. Anzai, N. *et al.* The multivalent PDZ domain-containing protein PDZK1 regulates transport activity of renal urate-anion exchanger URAT1 via its C terminus. *J. Biol. Chem.* **279,** 45942–45950 (2004).
26. Huls, M. *et al.* The breast cancer resistance protein transporter ABCG2 is expressed in the human kidney proximal tubule apical membrane. *Kidney Int.* **73,** 220–225 (2008).
27. Maliepaard, M. *et al.* Subcellular localization and distribution of the breast cancer resistance protein transporter in normal human tissues. *Cancer Res.* **61,** 3458–3464 (2001).
28. Doyle, L. A. & Ross, D. D. Multidrug resistance mediated by the breast cancer resistance protein BCRP (ABCG2). *Oncogene* **22,** 7340–7358 (2003).
29. Zaka, R. & Williams, C. J. New developments in the epidemiology and genetics of gout. *Curr. Rheumatol. Rep.* **8,** 215–223 (2006).
30. Wallace, S. L. *et al.* Preliminary criteria for the classification of the acute arthritis of primary gout. *Arthritis Rheum.* **20,** 895–900 (1977).
31. Puig, J. G. & Mateos, F. A. Clinical and biochemical aspects of uric acid overproduction. *Pharm. World Sci.* **16,** 40–54 (1994).
32. Perez-Ruiz, F., Calabozo, M., Erauskin, G. G., Ruibal, A. & Herrero-Beites, A. M. Renal underexcretion of uric acid is present in patients with apparent high urinary uric acid output. *Arthritis Rheum.* **47,** 610–613 (2002).
33. Wortmann, R. L. Gout and hyperuricemia. *Curr. Opin. Rheumatol.* **14,** 281–286 (2002).
34. Urano, W. *et al.* Sodium-dependent phosphate cotransporter type 1 sequence polymorphisms in male patients with gout. *Ann. Rheum. Dis.* **69,** 1232–1234 (2010).
35. The guideline revising committee of Japanese Society of Gout and Nucleic Acid Metabolism in *Guideline for the Management of Hyperuricemia and Gout* (ed. The guideline revising committee of Japanese Society of Gout and Nucleic Acid Metabolism) 60–72 (Medical Review, 2010).
36. Ichida, K. *et al.* Identification of two mutations in human xanthine dehydrogenase gene responsible for classical type I xanthinuria. *J. Clin. Invest.* **99,** 2391–2397 (1997).
37. Daimon, M. *et al.* Large-scale search of SNPs for type 2 DM susceptibility genes in a Japanese population. *Biochem. Biophys. Res. Commun.* **302,** 751–758 (2003).
38. Hayashi, H., Takada, T., Suzuki, H., Akita, H. & Sugiyama, Y. Two common PFIC2 mutations are associated with the impaired membrane trafficking of BSEP/ABCB11. *Hepatology* **41,** 916–924 (2005).
39. Takada, T., Weiss, H. M., Kretz, O., Gross, G. & Sugiyama, Y. Hepatic transport of PKI166, an epidermal growth factor receptor kinase inhibitor of the pyrrolo-pyrimidine class, and its main metabolite, ACU154. *Drug Metab. Dispos.* **32,** 1272–1278 (2004).
40. Hall, I. H., Scoville, J. P., Reynolds, D. J., Simlot, R. & Duncan, P. Substituted cyclic imides as potential anti-gout agents. *Life Sci.* **46,** 1923–1927 (1990).
41. Kitamura, Y. *et al.* Determination of probability distribution of diplotype configuration (diplotype distribution) for each subject from genotypic data using the EM algorithm. *Ann. Hum. Genet.* **66,** 183–193 (2002).

Acknowledgements

We express our gratitude to all the patients involved in this study. We thank T. Tamatsukuri, N. Katsuta and S. Terashige for genetic analysis; H. Fujiwara for patient analysis; and M. Yamashiro, K. Takahashi, T. Itoh, Y. Kobayashi and J. Fukuda for helpful discussion. This study was supported by grants from the Japan Society for the Promotion of Science, Ministry of Education, Culture, Sports, Science and Technology of Japan including Grant-in-Aid for Scientific Research on Innovative Areas HD-physiology (22136015), the Ministry of Health, Labour and Welfare of Japan, the Ministry of Defense of Japan, the Kawano Masanori Memorial Foundation for Promotion of Pediatrics, Takeda Science Foundation, and the Gout Research Foundation of Japan.

Author contributions

K. Ichida, H.M., T.T., M.H., N.S., T.H. and H.S. designed the experiment. K. Ichida, H.M., A.N., Y.T., Y.K., C.O., Y.U., M.N., Y. Shinohara and N.S. carried out genetic analysis. K. Ichida, H.M., A.N., T.S., H.I. and T.H. collected samples of patients and performed patient analysis. T.T., K.M., Y.Y., H.K.,Y.I., K. Ito and H.S. performed experimental analysis. H.N., T.N. and Y. S. performed statistical analysis. K. Ichida, H.M., T.T., A.N. and N.S. wrote the paper. K. Ichida, H.M. and T.T. contributed equally to this work.

Additional information

Supplementary Information accompanies this paper at http://www.nature.com/naturecommunications

Competing financial interests: K. Ichida, H.M., T.T., T.N., N.S., and H.S. have a patent pending based on the work reported in this paper (WO 2010/150525 A1, title: Urate transporter, as well as method and kit for evaluating urate transport-related disease factor and inflammation-related disease factor, and test sample and drug). Other authors declare no competing financial interests.

Reprints and permission information is available online at http://npg.nature.com/reprintsandpermissions/

How to cite this article: Ichida, K. *et al.* Decreased extra-renal urate excretion is a common cause of hyperuricemia. *Nat. Commun.* 3:764 doi: 10.1038/ncomms1756 (2012).

EUROPEAN JOURNAL OF PAEDIATRIC NEUROLOGY 17 (2013) 1–6

ELSEVIER

Official Journal of the European Paediatric Neurology Society

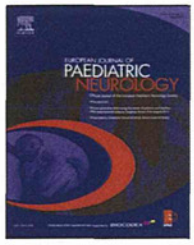

Review article

Molybdenum cofactor deficiency: Review of 12 cases (MoCD and review)

Erhan Bayram [a,*], *Yasemin Topcu* [a], *Pakize Karakaya* [a], *Uluc Yis* [a], *Handan Cakmakci* [b], *Kimiyoshi Ichida* [c], *Semra Hiz Kurul* [a]

[a] *Dokuz Eylul University Hospital, Department of Pediatrics, Division of Pediatric Neurology, 35340 Balcova, Izmir, Turkey*
[b] *Dokuz Eylul University Hospital, Department of Radiology, Izmir, Turkey*
[c] *Jikei University School of Medicine, Department of Internal Medicine, Division of Kidney and Hypertension, Tokyo, Japan*

ARTICLE INFO

Article history:
Received 15 August 2012
Received in revised form
7 October 2012
Accepted 13 October 2012

Keywords:
Molybdenum cofactor deficiency
Cystic encephalomalacia
Seizures
Feeding difficulty
Facial dysmorphism
Genes of molybdenum cofactor synthesis

ABSTRACT

Molybdenum cofactor deficiency is a rare inborn error of metabolism. The major clinical symptoms are intractable neonatal seizures, progressive encephalopathy, facial dysmorphic features and feeding difficulties. Most of the patients are misdiagnosed as hypoxic ischemic encephalopathy. The majority of patients have mutations in the MOCS1 and MOCS2 genes. Although the therapeutic treatment strategies have not been improved, genetic analysis is essential to elucidate the disease. Here, we report a review of 12 patients with Molybdenum cofactor deficiency reported from Turkey.

Contents

* *Corresponding author.* Tel.: +90 232 412 36 24; fax: +90 232 412 36 49.
E-mail address: dr.erhanbayram@yahoo.com (E. Bayram).
1090-3798/$ – see front matter
http://dx.doi.org/10.1016/j.ejpn.2012.10.003

1. Introduction

Molybdenum cofactor deficiency (MoCD) is an autosomal recessive disorder characterized by severe and progressive neurological deterioration, intractable seizures, facial dysmorphism, microcephaly and feeding difficulties.[1,2] MoCD leads to a combined deficiency of molybdenum cofactor dependent enzymes including xanthine dehydrogenase, sulphite oxidase, aldehyde oxidase and mitochondrial amidoxime reducing component.[3,4] MoCD mainly affects the central nervous system and may mimic hypoxic ischemic encephalopathy.[2] Global cerebral edema, cystic encephalomalacia, cortical and white matter atrophy, focal or bilateral changes within the globi pallidi and subthalamic regions, dysgenesis of corpus callosum and ventriculomegaly have been reported.[2,5] Majority of the mutations that caused the MoCD have been described in the genes of molybdenum cofactor synthesis step 1 (MOCS1) and molybdenum cofactor synthesis step 2 (MOCS 2) with two patients reported in gephrin (GPHN) gene.[6–8] Here, we report a 21 day old girl with MoCD, who was previously misdiagnosed as hypoxic ischemic encephalopathy, in whom a homozygous AG deletion in gene MOCS1 has been identified and review of the clinical, radiologic and genetic properties of the other 11 patients reported from Turkey.

2. A new case diagnosed with molybdenum cofactor deficiency

The patient was the second child of non-consanguineous parents. She was born after an uneventful pregnancy at 39 weeks of gestation. She had a three year old healthy sister. The weight, height and head circumferences at birth were 3500 g (50–75 p), 52 cm (25 p) and 36 cm (10–25 p), respectively. The APGAR scores were 5 at 1 min and 9 at 5 min. She was hypotonic and developed bradycardia and cyanosis. She was transferred to neonatal care unit and needed mechanical ventilation. On the second day of life, frequent multifocal myoclonic seizures started. The seizures were refractory to midazolam, phenobarbital and clonazepam. She was weaned from the ventilator on the fifth day of life but needed gavages feeding because of weak sucking. The cranial ultrasonography showed symmetric, diffuse periventricular white matter echogenicity. The patient was followed up with a diagnosis of hypoxic ischemic encephalopathy and on 21st day of life, the patient was transported to our hospital because of intractable seizures and feeding difficulties. On physical examination, she had severe truncal hypotonia with increased deep tendon reflexes. Suck reflex and swallowing was also poor. She also displayed some mild dysmorphic features like broad nasal bridge, high arched palate and prominent cheeks.

Laboratory investigations including liver and renal function tests, serum lactate, pyruvate, ammonia; urine, plasma and cerebrospinal fluid amino acid concentrations; TANDEM mass spectrometry; serum and cerebrospinal fluid glucose were normal. Serum uric acid levels obtained one week apart were 0.8 mg/dL and 0.3 mg/dL (2–5.5 mg/dL), respectively. Electroencephalography showed diffuse slowing of background activity and multifocal epileptiform activity. She had multifocal myoclonic seizures with a high pitch cry despite appropriate doses of phenobarbital, clonazepam, pyridoxine, pyridoxal 5 phosphate and folinic acid. Brain magnetic resonance imaging (MRI) findings on the 27th day of life revealed cerebral atrophy and multicystic encephalomalacia especially located in bilateral parieto-occipital regions (Fig. 1). Low serum uric acid levels with refractory seizures and radiologic findings suggested MoCD/sulfite oxidase deficiency. Fresh urine sulfite dipstick test was positive. Urinary levels of the S-sulphocysteine, xanthine and hypoxanthine were also high which favored the diagnosis of MoCD (Table 1). Ophtalmologic evaluation of the patient revealed no abnormality. The diagnosis was also confirmed by the genetic analysis which

Fig. 1 – T2 weighted axial image shows cerebral atrophy and multicystic encephalomalacia (arrows) especially located in bilateral frontoparieto-occipital regions.

Table 1 – Laboratory results of the patient.

Urine	Results mmol/mol creatinine	References mmol/mol creatinine
Taurine	998.32 ↑↑↑	16–226
S-sulphocysteine	249.35 ↑↑↑	0
Cysteine	4.28 ↓	5–53
Uric acide	77 ↓↓↓	443–695
Hypoxanthine	48 ↑	7–34
Xanthine	561 ↑↑↑	10–34
Plasma	**Results μmol/L**	**References μmol/L**
Cysteine	0 ↓↓↓	20–57
S-sulphocysteine	30.83 ↑↑↑	0

Table 2 – Summary of clinical, biochemical, radiologic and genetic findings for reported Turkish patients with molybdenum cofactor deficiency.

Case	Age at diagnosis (month)	Gender	Consanguinity	Clinical findings	Biochemical findings	Cranial MRI findings	Molecular genetics	Reference
1	3	M	No	Microcephaly, seizures, screaming episodes, feeding difficulties, triangular face	Plasma and urine urate ↓, urinary excretion of taurin and S-sulphocysteine ↑	Retrocerebellar cyst, diffuse cerebral, cerebellar atrophy, multiple cystic cavities and agenesis of cc	MOCS1 homozygous 217C > T, exon 5	Gumus et al. (2010)
2	30	F	Yes	Microcephaly, seizures, screaming episodes, feeding difficulties,	Plasma urate ↓, urinary excretion of xanthine ↑	Cerebral and cerebellar atrophy, multiple cystic cavities	MOCS1 homozygous c.667insCGA, exon 5	Sass et al. (2010)
3	2	M	Yes	Seizures, screaming episodes, feeding difficulties	Plasma urate ↓, urinary excretion of sulphite ↑ (dipstick test)	Cerebral atrophy, multiple cystic cavities, hypoplasia of the cerebellum	MOCS2 homozygous c.130C > T	Per et al. (2007)
4	1	F	Yes	Macrocephaly, coarse face, feeding difficulties, seizures	Metabolic acidosis, lactic acidosis, plasma urate ↓, urinary excretion of thiosulphate and sulphite (dipstick test) ↑, sulphite oxidase activity in skin fibroblast culture ↓	Hypoplasia of the cerebellum, Dandy Walker malformation, hypogenesis of the cc, intraventricular and intraparenchymal subacute hemorrhages, multicystic cavities	unknown	Teksam et al. (2005)
5	1	M	Yes	Feeding difficulties, seizures, broad nasal bridge, high arched palate	Plasma and urine urate ↓, plasma taurin↑, urinary excretion of sulphite, S-sulphocysteine, xanthine and hypoxanthine ↑	Cerebral atrophy, hypoplasia of cc and cerebellum, multiple cystic cavities, Dandy Walker malformation	unknown	Arslanoglu et al. (2001)
6	1	M	Yes	Seizures, coarse face	Plasma urate ↓, urinary excretion of thiosulphate and sulphite (dipstick test) ↑, sulphite oxidase activity in skin fibroblast culture↓	Multiple cystic cavities, dilated lateral ventricules, hyperintensity on T1-weighted images in the basal ganglia and thalami	unknown	Topcu et al. (2001)
7	1	M	No	Seizures, coarse face, micrognathia,	Plasma urate ↓, urinary excretion of S-sulphocysteine, xanthine, hypoxanthine, thiosulphate, sulphite (dipstick test) ↑, sulphite oxidase activity in skin fibroblast culture ↓	Hydrocephalic dilatation of the 3rd and lateral ventricles, cerebral atrophy, retrocerebellar cyst, hypoplasia of the vermis and cerebellum, hypoplasia of the cc, increased T1 signal intensity of the basal ganglia and thalami, cystic foci in the subcortical regions	unknown	Topcu et al. (2001)

(continued on next page)

Table 2 – (continued)

Case	Age at diagnosis (month)	Gender	Consanguinity	Clinical findings	Biochemical findings	Cranial MRI findings	Molecular genetics	Reference
8	1	F	Yes	Seizures, screaming episodes, microcephaly, feeding difficulties	Plasma urate ↓, urinary excretion of S-sulphocysteine, xanthine, thiosulphate and sulphite (dipstick test) ↑, sulphite oxidase activity in skin fibroblast culture ↓	Multiple cystic cavities, hypoplasia of the cc, cerebral and cerebellar atrophy, increased signal intensity on T1 weighted images in the bilateral thalami, enlarged cisterna magna	unknown	Topcu et al. (2001)
9	1	M	No	Seizures, coarse face, micrognathia,	Plasma urate ↓, urinary excretion of S-sulphocysteine, xanthine, hypoxanthine, thiosulphate and sulphite (dipstick test) ↑, urinary excretion of uric acid ↓, sulphite oxidase activity in skin fibroblast culture ↓	unknown	unknown	Coskun et al. (1998)
10	84	M	Yes	Mental-motor retardation, dystonic movements, spasticity, seizures,	unknown	unknown	MOCS1 c.666insCGA	Ichida et al. (2006)
11	13	M	No	Coarse face, seizures, opisthotonic postur, recurrent pneumonia, hematuria, feeding difficulties	Plasma urate ↓, plasma xanthine, hypoxanthine ↑, urinary excretion of uric acid ↓, urinary excretion of xanthine, hypoxanthine ↑,	Multicystic encephalomalacia, cerebral atrophy	unknown	Kavukcu et al. (2000)
12	1	F	No	Seizures, feeding difficulties, broad nasal bridge, high arched palate and prominent cheeks	Plasma cysteine↓, S-sulphocysteine↑ Urinary excretion of taurin, S-sulphocysteine, xanthine, hypoxanthine↑, cystein and urinary excretion of uric acid ↓	Multicystic encephalomalacia, cerebral atrophy	MOCS1 AG deletion	Our patient

cc, corpus callosum.

revealed a homozygous AG deletion in MOCS1 gene. At the age of three months, she had no head control, feeding difficulties and seizures of the patient continued.

3. Review of 12 patients reported from Turkey

Molybdenum cofactor deficiency is a rare inborn error of metabolism that was firstly described by Duran et al. in 1978.[9] Aldehyde oxidase, xanthine dehydrogenase, sulfite oxidase and mitochondrial amidoxime reducing component recently identified are molybdenum cofactor dependent enzymes and the absence of the cofactor leads to a combined deficiency of these four enzymes.[6] Patients with MoCD present with intractable seizures and feeding difficulties soon after birth. Patients develop severe psychomotor retardation due to progressive cerebral atrophy and ventricular dilatation. In some cases lens dislocation has also been described.[2] Molybdenum cofactor deficiency predominantly affects the central nervous system. The progression of the disease and underlying mechanisms of the progressive neurologic damage are not fully understood. It is considered that elevated levels of sulphite, taurine, S-sulphocysteine and thiosulphate are related with the progressive central nervous system toxicity.[10] Major radiological features of the disease include multicystic white matter lesions, symmetrical involvement of the globi pallidi, pontocerebellar hypoplasia with retrocerebellar cyst, Dandy Walker complex and dysgenesis of corpus callosum.[2,11,12] Our patient was also presented with intractable seizures and feeding difficulties in the early newborn period and brain MRI revealed cerebral atrophy and multicystic encephalomalacia especially located in bilateral parieto-occipital regions.

Isolated sulphite oxidase deficiency is clinically very similar to MoCD. Fresh urine strip test which has been developed to measure the sulphite concentrations is positive in both diseases. These two disorders can be differentiated by biochemical analysis. In patients with isolated sulphite oxidase deficiency and MoCD, sulphite levels are elevated and lead to an accumulation of the S-sulphocysteine. Elevated levels of thiosulphate and taurine may also be observed in both disorders. Additionally in MoCD, excretion of the xanthine and hypoxanthine in urine are elevated due to the abnormal xanthine dehydrogenase pathway. Our patient's urine sample also showed elevated levels of S-sulphocysteine, xanthine and hypoxanthine (Table 1).

MOCS1, MOCS2 and GPHN genes are essential for the synthesis of molybdenum cofactor. MOCS1 and MOCS2 have an unusual bicistronic architecture, have identical very low expression profiles, and show extremely conserved C-terminal ends in their 5-prime open reading frames. MOCS1 mutations are responsible for two-thirds of cases. MOCS1 and MOCS2 mutations affect one or several highly conserved motifs and no missense mutations of a less conserved residue were identified. Only two patients with GPHN mutations have been described.[7,8] We identified a homozygous AG deletion in MOCS1 gene in our patient.

More than 100 patients have been reported from diverse ethnic groups. It is possible that the incidence of the disease is higher than reported as a result of misdiagnosed patients. Common clinical findings were intractable seizures, feeding difficulties, severe developmental delay and death early in life.[2,13] In rarity of the reported patients Mize et al described a patient with a diagnosis of MoCD and Marfan-like habitus and Boles et al reported a MoCD patient with lactic acidosis.[14,15] Despite the clinical investigations, effective treatment strategies have not been improved yet.[1,16] Recently, Veldman et al reported that intravenous administration of cyclic pyranopterin monophosphate (cPMP) may resolves the metabolic abnormalities and showed valuable clinical improvement.[1]

To the best of our knowledge, eleven Turkish patients with MoCD have been reported in the literature. The mean age at the diagnosis was 12.5 months. Eight (72.7%) of the patients were male and there was history of consanguinity in seven of them (63.6%). The most common clinical findings were intractable seizures, feeding difficulties, dysmorphic facies and screaming episodes.[11–13,17–20] Some of the patients had atypical findings like macrocephaly, metabolic acidosis, lactic acidosis and hematuria.[18,19] Neuroimaging findings of the patients revealed multicystic cerebral lesions, cerebral and cerebellar atrophy, dysgenesis of corpus callosum, Dandy Walker malformation, retrocerebellar cyst, dilated ventricles and increased signal intensities in the thalami.[11–13,17–19] Three patients had mutation in MOCS1 gene and one patient had mutation in MOCS2 gene.[11,13,17,22] The diagnosis of the remaining patients (7/11 (63.6%)) were confirmed by biochemical analysis or decreased sulphite oxidase activity in skin fibroblast culture.[12,18–21] The laboratory and genetic analysis results of the patients were summarized in the Table 2.

In conclusion, MoCD should be considered in the differential diagnosis of hypoxic ischemic encephalopathy who present with intractable seizures and feeding difficulties. Multicystic cerebral lesions and decreased levels of uric acid in serum and urine provide clues for the diagnosis. Molecular genetic analysis of the related gene should be performed to elucidate the disease and families must undergo precise genetic counseling.

REFERENCES

1. Veldman A, Santamaria-Araujo JA, Sollazzo S, et al. Successful treatment of molybdenum cofactor deficiency type A with cPMP. *Pediatrics* 2010;**125**:1249–54.
2. Vijayakumar K, Gunny R, Grunewald S, et al. Clinical neuroimaging features and outcome in molybdenum cofactor deficiency. *Pediatr Neurol* 2011;**45**:246–52.
3. Schwartz G, Mendel RR, Ribbe MW. Molybdenum cofactors, enzymes and pathways. *Nature* 2009;**460**:839–47.
4. Havemeyer A, Lang J, Clement B. The fourth mammalian molybdenum enzyme mARC: current state of research. *Drug Metab Rev* 2011;**43**:524–39.
5. Carmi-Nawi N, Malinger G, Mandel H, Ichida K, Lerman-Sagie T, Lev D. Prenatal brain disruption in molybdenum cofactor deficiency. *J Child Neurol* 2011;**26**:460–4.
6. Reis J, Johnson JL. Mutations in the molybdenum cofactor biosynthetic genes MOCS1-MOCS2 and GEPH. *Hum Mutat* 2003;**21**:569–76.
7. Reiss J, Gross-Hardt S, Christensen E, Schmidt P, Mendel RR, Schwarz G. A mutation in the gene for the neurotransmitter

receptor-clustering protein gephyrin causes a novel form of molybdenum cofactor deficiency. *Am J Hum Genet* 2001;**68**:208–13.
8. Reiss J, Lenz U, Aquaviva-Bourdain C, Joriot-Chekaf S, Mention-Mulliez K, Holder-Espinasse M. A GPHN point mutation leading to molybdenum cofactor deficiency. *Clin Genet* 2011;**80**:598–9.
9. Duran M, Beemer FA, van de Heiden C, et al. Combined deficiency of xanthine oxidase and sulphite oxidase: a defect of molybdenum metabolism or transport? *J Inherit Metab Dis* 1978;**1**:175–8.
10. Abbas AK, Xia W, Tranberg M, Wigstrom H, Weber SG, Sandberg M. S sulfocysteine is an endogenous amino acid in neonatal rat brain but an unlikely mediator of cysteine neurotoxicity. *Neurochem Res* 2008;**33**:301–7.
11. Gümüş H, Ghesquiere S, Per H, et al. Maternal uniparental isodisomy is responsible for serious molybdenum cofactor deficiency. *Dev Med Child Neurol* 2010;**52**:868–72.
12. Arslanoglu S, Yalaz M, Gökşen D, et al. Molybdenum cofactor deficiency associated with Dandy-Walker complex. *Brain Dev* 2001;**23**:815–8.
13. Sass JO, Gunduz A, Araujo Rodrigues Funayama C, et al. Functional deficiencies of sulfite oxidase: differential diagnoses in neonates presenting with intractable seizures and cystic encephalomalacia. *Brain Dev* 2010;**32**: 544–9.
14. Mize C, Johnson JL, Rajagopalan KV. Defective molybdopterin biosynthesis: clinical heterogeneity associated with molybdenum cofactor deficiency. *J Inherit Metab Dis* 1995;**18**:283–90.
15. Boles RG, Ment LR, Meyn MS, Horwich AL, Kratz LE, Rinaldo P. Short-term response to dietary therapy in molybdenum cofactor deficiency. *Ann Neurol* 1993;**34**:742–4.
16. Schwarz G, Santamaria-Araujo JA, Wolf S, et al. Rescue of lethal molybdenum cofactor deficiency by a biosynthetic precursor from Escherichia coli. *Hum Mol Genet* 2004;**13**:1249–55.
17. Per H, Gümüş H, Ichida K, Cağlayan O, Kumandaş S. Molybdenum cofactor deficiency: clinical features in a Turkish patient. *Brain Dev* 2007;**29**:365–8.
18. Teksam O, Yurdakok M, Coskun T. Molybdenum cofactor deficiency presenting with severe metabolic acidosis and intracranial hemorrhage. *J Child Neurol* 2005;**20**:155–7.
19. Topcu M, Coskun T, Haliloglu G, Saatci I. Molybdenum cofactor deficiency: report of three cases presenting as hypoxic-ischemic encephalopathy. *J Child Neurol* 2001;**16**:264–70.
20. Coşkun T, Yetük M, Yurdakök M, Tekinalp G. Blood uric acid as a pointer to the diagnosis of molybdenum cofactor deficiency. *Acta Paediatr* 1998;**87**:714–5.
21. Kavukçu S, Soylu A, Sahin B, Türkmen M, Aydin A, Dirik E. Clinical quiz. Molybdenum cofactor deficiency. *Pediatr Nephrol* 2000;**14**:1145–7.
22. Ichida K, Aydin HI, Hosoyamada M, et al. Turkish case with molybdenum cofactor deficiency. *Nucleosides Nucleotides Nucleic Acids* 2006;**25**:1087–91.

Int. J. Mol. Sci. **2012**, *13*, 15475-15495; doi:10.3390/ijms131115475

OPEN ACCESS
International Journal of
Molecular Sciences
ISSN 1422-0067
www.mdpi.com/journal/ijms

Review

Mutations Associated with Functional Disorder of Xanthine Oxidoreductase and Hereditary Xanthinuria in Humans

Kimiyoshi Ichida [1], Yoshihiro Amaya [2], Ken Okamoto [3] and Takeshi Nishino [3,4,*]

1 Department of Pathophysiology, Tokyo University of Pharmacy and Life Sciences 1432-1, Horinouchi, Hachioji, Tokyo 192-0392, Japan; E-Mail: ichida@toyaku.ac.jp
2 Division of Biochemistry, Niigata University Graduate School of Medical and Dental Sciences, 2-5274 Gakkocho-dori, Chuo-ku, Niigata 951-8514, Japan; E-Mail: amaya@dent.niigata-u.ac.jp
3 Department of Biochemistry and Molecular Biology, Nippon Medical School, 1-1-5 Sendagi, Bunkyou-ku, Tokyo 113-8602, Japan; E-Mail: okamoto@nms.ac.jp
4 Department of Applied Biological Chemistry, Graduate School of Agricultural and Life Sciences, University of Tokyo, 1-1-1 Yayoi, Bunkyo-Ku, Tokyo 113-8657, Japan

* Author to whom correspondence should be addressed; E-Mail: nishino@nms.ac.jp; Tel.: +81-3-5841-5165; Fax: +81-3-5841-8023.

Received: 7 October 2012; in revised form: 26 October 2012 / Accepted: 29 October 2012 / Published: 21 November 2012

Abstract: Xanthine oxidoreductase (XOR) catalyzes the conversion of hypoxanthine to xanthine and xanthine to uric acid with concomitant reduction of either NAD^+ or O_2. The enzyme is a target of drugs to treat hyperuricemia, gout and reactive oxygen-related diseases. Human diseases associated with genetically determined dysfunction of XOR are termed xanthinuria, because of the excretion of xanthine in urine. Xanthinuria is classified into two subtypes, type I and type II. Type I xanthinuria involves XOR deficiency due to genetic defect of XOR, whereas type II xanthinuria involves dual deficiency of XOR and aldehyde oxidase (AO, a molybdoflavo enzyme similar to XOR) due to genetic defect in the molybdenum cofactor sulfurase. Molybdenum cofactor deficiency is associated with triple deficiency of XOR, AO and sulfite oxidase, due to defective synthesis of molybdopterin, which is a precursor of molybdenum cofactor for all three enzymes. The present review focuses on mutation or chemical modification studies of mammalian XOR, as well as on XOR mutations identified in humans, aimed at understanding the reaction mechanism of XOR and the relevance of mutated XORs as models to estimate the possible side effects of clinical application of XOR inhibitors.

Keywords: xanthine dehydrogenase; xanthine oxidase; xanthine oxidoreductase; xanthine oxidoreductase deficiency; flavoproteins; xanthinuria; hereditary xanthinuria; gout

1. Introduction

Xanthine oxidoreductase (XOR) catalyzes two hydroxylation steps in the metabolic pathway of purine degradation, *i.e.*, hypoxanthine to xanthine and xanthine to uric acid, utilizing either NAD^+ or O_2 [1–3] (Figure 1). In higher animals, XOR exists as a homodimer of 150 kDa subunits [4]. Each subunit contains one molybdenum center (molybdenum cofactor; Moco), one flavin adenine dinucleotide (FAD) cofactor and two distinct iron sulfur centers ([2Fe-2S] type) [1–3]. The purine hydroxylation reaction occurs at the molybdenum center. Electrons, which are transferred to molybdenum during the hydroxylation reaction, are further transferred to FAD via the two iron sulfur centers [5,6]. Finally, NAD^+ or oxygen molecule, which is the final electron acceptor, is reduced at the FAD center.

Figure 1. Metabolic pathways of purine degradation in humans. Xanthine oxidoreductase (XOR) catalyzes the transformations of hypoxanthine to xanthine and xanthine to uric acid. XOR-deficient patients secrete xanthine, which is formed from guanine. Accumulated hypoxanthine is mostly converted to inosine monophosphate (IMP) via the salvage pathway using 5-phospho-α-D-ribosyl 1-pyrophosphate (PRPP) as a co-substrate.

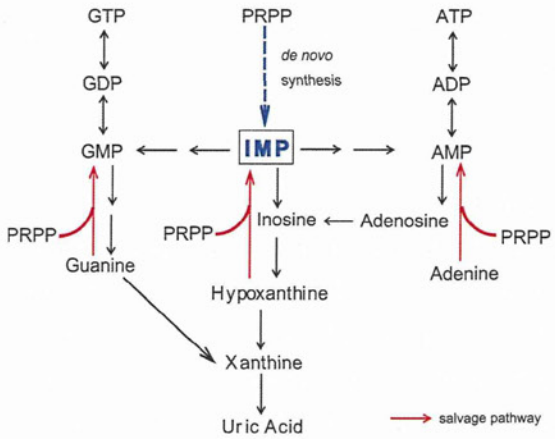

XOR has two forms: xanthine dehydrogenase (XDH), which prefers NAD^+ as the substrate and xanthine oxidase (XO), which prefers O_2 [1]. Historically, XDH and XO have been studied as distinct enzymes. XOR has been isolated only as the XO form from mammalian sources, whereas it has always been purified in the XDH form from other organisms [2]. It is becoming clear, however, that mammalian XORs exist in the XDH form under normal conditions in the cell, but are converted to the XO form during extraction or purification, either irreversibly by proteolysis or reversibly by oxidation of cysteine residues to disulfide bridges. In some particular cases, XDH can be converted to the XO form [2]. The mechanism of conversion from XDH to XO has been thoroughly elucidated in the past decade by means of a range of techniques, including X-ray crystal structure analysis of various mutants, and it has become clear that the protein environment influences the reactivity of the FAD

cofactor towards different substrates through substantial conformational changes triggered by modifications located far from the cofactor [5,6].

The enzyme is a target of drugs to treat hyperuricemia, gout or reactive oxygen-related diseases [7,8]. It is distributed in various organs including liver, mammary gland and endothelial cells of vascular vessels [9,10]. The enzyme was proposed to be localized in peroxisomes of rat liver [11], but was found to be present in cytosol [12]. As XOR inhibitors significantly lower uric acid production and concentration in the blood, they can be used to treat gout. Allopurinol, which was introduced by Elion *et al.* [13], has been on the market for over 40 years [14]. In recent years, however, several companies have developed very effective inhibitors [14–16], of which one example is febuxostat [17]. Clinical trials indicate that febuxostat is superior to allopurinol in lowering uric acid production, although the mechanism of inhibition is different [18,19]. By means of enzymatic, spectroscopic and structural-biological analyses of the inhibition mechanism, it has been shown that these recently developed inhibitors bind tightly to both the oxidized and reduced forms of XOR in a highly structure-specific manner [15], whereas allopurinol, a substrate analogue, binds covalently to the reduced molybdenum atom (MoIV) after having been converted to the hydroxylated product (oxipurinol: alloxanthine) [20], mimicking the reaction intermediate formed during the hydroxylation reaction with xanthine as a substrate [21]. Although oxipurinol binds very tightly to the enzyme, it can be dissociated from the molybdenum (VI) by spontaneous reoxidation due to electron transfer to other centers with a half-time of 300 min at 25 °C [20]. Potent inhibition seems to be essential to lower the uric acid level in blood or tissue, since XOR is a house-keeping enzyme that exists abundantly in various organs [10]. However, it has been suggested that lowering uric acid levels may cause side effects in humans, since uric acid acts as a radical scavenger in the body [22,23]. Further, it is proposed that NO formed by XOR via reduction of NO_2 (with any electron donor) may induce vasodilatation under ischemic conditions [24–26]. On the other hand, XOR has the potential to generate oxygen radical species (H_2O_2 and O_2^-) after conversion from XDH to XO [1–6]. O_2^- would rapidly react with NO to form $ONOO^-$ [27]. This reaction may serve to eliminate NO, at least in part, but the $ONOO^-$ produced is highly toxic [28]. As to the question of potential NO formation by XOR, the activity for NO formation from NO_2 is extremely low, even under anaerobic conditions, although from a chemical point of view it is possible that the water-exchangeable hydroxyl group at OH-Mo(IV) can be replaced by NO_2 to produce NO, since various compounds, such as uric acid (which reacts very slowly to form xanthine), can behave similarly, as discussed by Okamoto [29]. The reported k_{cat} value of NO formation is 0.17 s^{-1} at 37 °C with NADH as an electron donor under anaerobic conditions [30], *i.e.*, less than 1% of k_{cat} for xanthine oxidizing activity (k_{cat} value 15–20 s^{-1} at 25 °C) [31,32]. It is questionable whether such a weak activity can have any physiological significance, even under ischemic conditions. The present review focuses mainly on mutational studies of XOR and mutations associated with hereditary dysfunction of XOR in humans, since these are useful for understanding the enzyme reaction mechanism and also as models to estimate the possible side effects of using XOR inhibitors as drugs.

2. Symptoms of XOR Deficiency and Differential Diagnosis

Human diseases associated with genetic dysfunction of XOR are termed xanthinuria, because xanthine is excreted in the urine [33]. Although the enzyme catalyzes two steps of reaction, as described above, so that XOR dysfunction might be expected to be associated with tissue accumulation of hypoxanthine due to inhibition of the first step (conversion of hypoxanthine to xanthine), in fact hypoxanthine is not normally significantly excreted in urine [34,35]. Instead, hypoxanthine is converted to inosine monophosphate (IMP) owing to activation of the salvage pathway (Figure 1) [36]. Patients typically have low levels of uric acid (less than 1 mg/dL) in blood, so XOR-deficient patients are frequently identified based on measurement of uric acid in blood. Various diseases or disorders other than xanthinuria may lead to hypouricemia (Table 1). Renal hypouricemia, which can be caused by decreased re-absorption due to impaired function of urate transporter in the nephrons, is also clinically asymptomatic in most cases.

Table 1. Causes of hypouricemia.

Inherited disorders of purine metabolism
Genetic defects in the molybdoflavoprotein enzymes:
Xanthinuria type I (xanthine oxidoreductase deficiency)
Xanthinuria type II (molybdenum cofactor sulfurase deficiency: combined xanthine oxidoreductase and aldehyde oxidase deficiencies)
Molybdenum cofactor deficiency
Purine nucleoside phosphorylase deficiency
Phosphoribosylpyrophosphate synthetase deficiency
Secondary reduction in uric acid biosynthesis
Hepatic failure
Inherited renal hypouricemia (isolated renal tubule reabsorption defect)
Renal hypouricemia-1 [URAT1 (SLC22A12) deficiency]
Renal hypouricemia-2 [URAT9 (SLC22A9) deficiency]
Inherited causes of the Fanconi renotubular syndrome and its variants (the syndrome of multiple renal tubule reabsorption defects)
Fanconi renotubular syndrome 1
Cystinosis (accumulation of intralysosomal cystine)
Galactosemia (galactose-1-phosphate uridylyltransferase deficiency)
Hereditary fructose intolerance (fructose 1-phosphate aldolase B deficiency)
Glycogen storage disease type 1 (glucose-6-phosphate deficiency)
Wilson's disease [ATPase, Cu^{2+} transporting, beta polypeptide (ATP7B) deficiency]
Mitochondrial complex IV deficiency (cytochrome c oxidase deficiency)
Acquired causes of the Fanconi renotubular syndrome and its variants
Metal poisoning (e.g., Cd, Zn, Cu, Pb, Hg)
Multiple myeloma
Nephrotic syndrome
Malignant disease
Autoimmune disease (e.g., Sjogren's syndrome)
Thermal burns
Primary hyperparathyroidism

Table 1. *Cont.*

Acquired causes of the Fanconi renotubular syndrome and its variants
Acute renal tubular necrosis
Renal transplant rejection
Drugs
Xanthine oxidoreductase inhibitor (e.g., allopurinol, febuxostat)
Drugs used either as uricosuric agents or to block other aspects of renal tubule excretion (e.g., sulfinpyrazone, probenecid, benzbromarone)
Non-steroidal anti-inflammatory drugs with uricosuric properties (e.g., phenylbutazone, azapropazone, high dose of aspirin)
Coumarin anticoagulants (e.g., warfarin)
Outdated tetracycline (5 alpha-6-anhydro-4-epitetracycline)
Nutritional deficiencies
Vitamines B_{12}, C, D
Kwashiorkor

Xanthinuria is classified into two subtypes, type I and type II (Table 1) [35]. The type I is due to a genetic defect of XOR, whereas the type II is due to a genetic defect in molybdenum cofactor sulfurase [37,38]. Aldehyde oxidase (AO), also a molybdoflavo enzyme, is similar to XOR. A terminal sulfide group is necessary as the third ligand in the active center of XOR and AO for enzymatic activation of these enzymes after biosynthesis of the molybdenum cofactor. Molybdenum cofactor sulfurase catalyzes this final maturation step by generating a protein-bound persulfide, which is the source of the terminal sulfur ligand of the molybdenum cofactor. Thus, lack of sulfurase results in type II xanthinuria. Type I and II xanthinuria are not clinically distinguishable. In order to differentiate them, allopurinol loading test and gene analysis are performed, because a measurement method for molybdenum cofactor sulfurase activity has not yet been established [39,40]. In the allopurinol loading test, oxipurinol is detected in serum and urine of type I xanthinuria patients after administration of allopurinol, as conversion of allopurinol to oxipurinol is catalyzed by XOR and AO, while oxipurinol is not detected in the case of type II xanthinuria. AO has broad substrate specificity, oxidizing different types of aldehydes and heterocyclic rings [41,42]. No clinical symptom or abnormal laboratory examination result due to lack of AO has yet been identified. However, it has recently been reported that AO plays an important role in the metabolism of numerous compounds. Thus, classification of type I and II xanthinuria might be indispensable for optimum medical treatment of patients with xanthinuria in the future.

In higher animals other than primates, xanthinuria is lethal due to kidney damage resulting from xanthine stones in the urinary tract [43–46]. Although primates have lost uricase during evolution and seem to have acquired tolerance to oxipurines, e.g., through downregulation of XOR gene expression, other animals convert uric acid to more soluble allantoin, catalyzed by peroxisomal uricase, and do not seem to have such tolerance [47]. Urolithiasis is sometimes accompanied with xanthinuria due to xanthine deposition, and rarely this may lead to acute renal failure [48–53]. In addition to its role in uric acid production, XOR has bactericidal activity via ROS generation under certain conditions, particularly in mammalian mammary gland [54]. In addition to the NO_2 reduction as described in the previous section, XOR has been proposed to play a role in lactation, though the mechanism of the role

in lactation remains unclear [55,56]. XOR has also been suggested to be implicated in hypertension, cardiovascular disorder, and adipogenesis [57,58]. Although the situation is not simple, clinical observations in xanthinuria patients with extremely low serum uric acid levels, who show no symptoms, suggest that administration of XOR inhibitors may not cause severe side effects if the inhibitor has no other effect than inhibition of XOR, except possibly in special cases, such as cancer, pregnant or breast-feeding patients. Many purine analogue cancer drugs, such as mercaptopurine, are known to be catabolized by XOR [59]. The third type of XOR deficiency, type III XOR deficiency, involves the molybdenum cofactor. Molybdenum cofactor deficiency involves triple deficiency of XOR, AO and SO (sulfite oxidase), due to a defect in the synthesis of molybdopterin, which is a precursor of molybdenum cofactor for all three enzymes. Symptoms of molybdenum cofactor deficiency include severe neurological disorder, lens dislocation and dysmorphism, and the outcome is poor [60].

3. Overall Structure of Human Xanthine Oxidoreductase (XOR)

The primary structure of human XOR was first reported by Ichida *et al.* [61], who isolated cDNA clones encoding human *XOR* by cross hybridization with rat cDNA, the structure of which was reported by Amaya in 1990 [62]. The *XOR* gene has 36 exons, and is located in chromosome 2p23.1 [63,64]. The primary structure of human XOR has 90% homology with the rat enzyme over the entire length. Although cloning of human XOR was subsequently reported by several groups [64–66], the sequences were all very similar, except for one reported by Wright et al that was later found to encode AO, not XOR. Although mammalian XORs and AOs from various sources have similar molecular weights and cofactors [2,6,67], their substrate specificities are different. AO exclusively utilizes O_2 as the oxidizing substrate rather than NAD^+, which is used by dehydrogenases. The specificities of the two enzymes for reducing substrates partially overlap, and each is capable of hydroxylating a distinct subset of a wide range of aldehydes and aromatic heterocycles. Purine bases are good substrates of XORs, but are not good substrates of AOs. The physiological substrates of mammalian AOs are not known, although the involvement of AOs in drug metabolism is well-established [42]. Structure-based sequence comparisons have identified residues in the vicinity of the active site molybdenum center of AO that differ from those in XOR, and these are most probably the determinants of the substrate preferences exhibited by the family members [68]. However, a glutamic acid residue, thought to represent an essential catalytic base, is strictly conserved in AOs and XORs, pointing to a common catalytic mechanism for all family members [69].

The crystal structures of human XOR from natural milk at 3.6 Å resolution (PDB: 2CKJ) and recombinantly produced XDH at 2.6 Å resolution (PDB: 2E1Q) [69] are available. Higher resolution structures of mammalian XORs are available for native bovine XDH and XO, as well as recombinantly produced rat XDH and XO, including various mutants [69,70]. The subunits in the crystal structures of all these mammalian XORs are arranged as identical dimers that display a distinct butterfly shape [4,69,70]. The dimensions of the whole enzyme molecule are about 155 Å × 90 Å × 70 Å (Figure 2). Each monomer is composed of three subdomains. The small *N*-terminal domain (residues 1 to 165 in the human enzyme) contains both of the iron-sulfur centers (Fe/S I and Fe/S II) and is connected to the second, FAD-containing domain (residues 226 to 532, colored light green in Figure 1)

via a long, partially disordered segment consisting of residues 166 to 225. The FAD domain, in turn, is connected to the third, *C*-terminal domain via another extended segment (residues 533 to 590), which is also partially disordered. The third and largest domain (residues 591 to 1317, colored light blue in Figure 2) binds Moco close to the interface of the Fe/S- and FAD-binding domains, connected with a *C*-terminal loop (residues 1318–1333, colored blue in Figure 2) [4,69,70].

Figure 2. Structure of human XOR. The structure illustrated is that of a human mutant dimeric XDH [69] (PDB: 2E1Q). The Fe/S, FAD, and molybdopterin domains are colored light pink, light green and light blue, respectively. The interdomain loop (residues 533–590) is colored red. *C*-terminal is colored blue. A schematic representation of the domain structure in relation to the primary sequence is shown at the bottom.

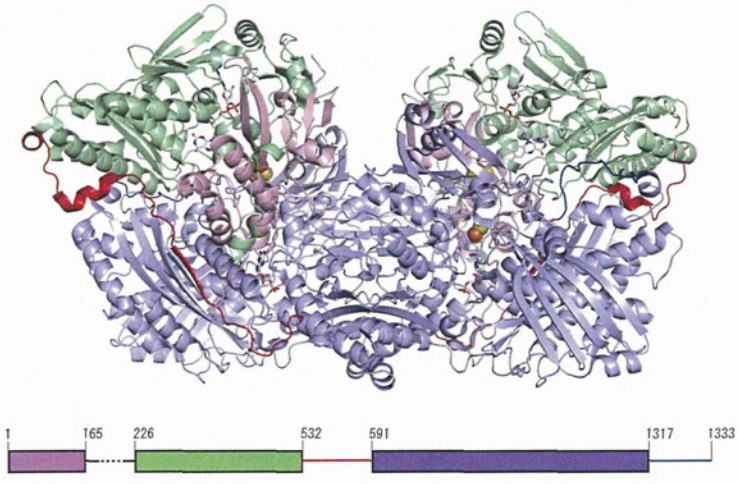

4. Residues Crucial for Enzyme Function: Experimental Studies

In order to elucidate the mechanisms of hydroxylation at the molybdenum center, electron transfer within the redox centers and reoxidation of the reduced FAD by the natural substrate, NAD^+ or molecular oxygen, various chemical modification and mutation studies have been performed during the last two decades. The amino acid residues of human XOR corresponding to those that have so far been found to be crucial for enzyme function, either by chemical modification or by mutagenesis studies with bovine or rat XORs, are summarized in Table 2.

Table 2. Residues crucial for enzyme function revealed by experimental studies.

Corresponding human residue No.	Residue in experimental animal	Function	Experiments
The Fe/S domain			
Cys43	rat Cys43	Fe/S II ligand	mutation to Ser [71]
Cys51	rat Cys51	Fe/S II ligand	mutation to Ser or Ala [71]
Cys116	rat Cys115	Fe/S I ligand	mutation to Ser [71]
Lys185	rat Lys184	interdomain	Trypsin [62]

Table 2. *Cont.*

Corresponding human residue No.	Residue in experimental animal	Function	Experiments
		The FAD domain	
Arg427	bovine Arg427	A member of the cluster XDH/XO conversion	mutation to Gln [72]
Arg335	bovine Arg335	A member of the cluster XDH/XO conversion	mutation to Ala [72]
Trp336	bovine Trp336 & rat Trp335	A member of the cluster XDH/XO conversion	mutation to Ala [72]
Phe337	rat Phe336	redox potential of FAD	mutation to Leu (to be published)
Tyr393	chicken Tyr419	NAD^+ binding	chemical modification with FSBA [73]
Asp429	rat Asp428	redox potential of FAD	mutation (to be published)
Cys536	rat Cys535	disulfide formation with Cys992 XDH/XO conversion	mutation to Ala [70] & chemical modification with FDNB [74]
Lys552	rat Lys551	Interdomain trypsin XDH/XO	Trypsin [62]
		The Moco domain	
Lys755	bovine Lys754	k_{cat} slower	chemical modification with FDNB [74,75]
Lys772	bovine Lys771	k_{cat} slower	chemical modification with FDNB [74,75]
Glu803	human	purine binding	mutation to Val [69]
Arg881	human	purine binding	mutation to Met [69]
Cys993	rat Cys992	disulfide with Cys535 XDH/XO conversion	mutation to Arg [70] & chemical modification with FDNB [74]
Glu1262	human		mutation to Ala [69,76]
Cys1318	rat Cys1316	disulfie with Cys1324?	mutation to Ser [70]
Cys1326	rat Cys1324	disulfide with Cys1316?	mutation to Ser [70] & chemical modification with FDNB [74]

4.1. The N-*Terminal Fe/S Domain*

This domain contains a cluster of two distinct [2Fe-2S] types, having different EPR signals and redox potentials, and these are named the Fe/S I and Fe/S II centers [77–79]. The Fe/S I signal displays *g*-values of $g_{1,2,3}$ = 2.022, 1.932, 1.894, with line-widths and relaxation properties typical of a [2Fe-2S] cluster, while Fe/S II has g-values of $g_{1,2,3}$ = 2.110, 1.991, 1.902, with unusually broad line widths and relaxation properties. The latter signals can only be observed below 25 K [80]. Site-directed mutagenesis studies employing heterologously expressed rat XOR have allowed assignment of the two distinct types of EPRsignals to the respective clusters [71], with Fe/S I being located in the unusual-^{113}Cys-Xaa$_2$-^{116}Cys-//-^{148}Cys-Xaa$_1$-^{15} Cys-motif in the α-helical domain and Fe/S II in the *N*-terminal-^{43}Cys-X-^{48}Cys-X-^{51}Cys-//-^{73}Cys-motif in the ferredoxin-like domain. This establishes the sequence of electron transfer within the enzyme molecule as Mo → Fe/S I → Fe/S II → FAD. It was noted that the mutation at Cys43Ser or Cys51Ala, which are both components of Fe/S I, resulted in the appearance of insoluble or monomeric proteins, suggesting the importance of the Fe/S I cluster for protein conformation and/or folding [71].

4.2. The Intermediate FAD Domain

The domain binds its cofactor FAD in a deep cleft; in the NAD-free form, the *si*-face of the isoalloxazine ring is exposed to solvent (Figure 3). The same space allows the substrate NAD access to the flavin, and the two ring systems stack on top of each other [81]. Modification of the chicken XDH residue corresponding to Tyr419 (human Tyr393) with fluorosulfonylbenzoyl adenosine (FSBA) resulted in loss of activity towards NAD^+ [73], suggesting that this tyrosine residue is indeed involved in NADH binding, as indicated by the crystal structure of the rat XDH-NADH complex (Tomoko Nishino, K. Okamoto, E.F. Pai and Takeshi Nishino, unpublished data). In contrast to the open *si*-side, the *re*-side of the flavin ring is in tight contact with residues of the protein chain, e.g., the side chain of Phe336 (human Phe337) lies parallel to the isoalloxazine ring. Mutation study indicated that this phenyl-flavin pair may serve to tune the cofactor's FAD redox potential (Tomoko Nishino, K. Okamoto, E.F. Pai and Takeshi Nishino, unpublished data). In the crystal structures of XDH and XO, the location of so-called loop A (residues 423–433 in human XOR) is very different in rat and bovine XORs. In rat and bovine XDH, the side chain of Asp428 (rat sequence, corresponding to human & bovine Asp429) in the loop is close to C_6 of the flavin. This residue must be a major contributor to the strong negative charge at the flavin-binding site [4,81]. Mutation of this residue with rat XOR changes the reactivity of FAD by changing its redox potential (Y. Kawaguchi *et al.* unpublished). In XO conformation, Asp428 moves away from the flavin ring and the guanidinium group of Arg425 replaces it, approaching the nearest atom of the isoalloxazine ring to within 6.3 Å. This reversal of the electrostatic potential surrounding the redox-active part of the FAD cofactor matches predictions based on biochemical and biophysical studies of the XDH and XO forms [82–84]. Bovine Arg427, Arg335, Trp336 and Phe549 (human Arg335, Trp336, Arg427 and Phe550) are components of a unique cluster of four amino acids [72], which are held together mostly via π-cation interactions in the XDH form. Phe549 (rat Phe549, human Phe550) is located in the long linker between the intermediate FAD and *C*-terminal Moco domains. In the XO form, however, this cluster is disrupted (Figure 3) [5]. An equivalent effect can be achieved by mutating one of these residues with rat XOR [72]. Proteolysis at Lys551 (human Lys552) [62], leading to drastically increased mobility of the linker peptide between the intermediate FAD and *C*-terminal Moco domains, or disulfide formation between Cys535 and Cys992 [70,74], causing conformational strain, breaks Phe549 out of this tight arrangement. Disruption of the cluster is accompanied with movement of the active site loop A. Recent studies suggest that the conversion from XDH to XO is in equilibrium [85]; the highly packed amino acid cluster, binding of NAD^+/NADH and insertion of the *C*-terminal peptide shift the equilibrium towards the XDH form, while disulfide formation between Cys535 and Cys992 (human Cys536 and Cys993) or proteolysis in the linker between the FAD and the Moco domains disrupts the amino acid cluster and moves the active site loop A. In rat enzyme extrusion of the C-terminal peptide, by formation of a disulfide bond between Cys1316 and Cys1324, shifts the equilibrium partially to the XO form.